JAAS

PAPER

View Article Online
View Journal | View Issue

Cite this: *J. Anal. At. Spectrom.*, 2023, **38**, 1421

Development and industrial application of LIBS-XRF coal quality analyzer by combining PCA and PLS regression methods

Zhihui Tian,[ab] Jiaxuan Li,[ab] Shuqing Wang,[c] Yu Bai,[d] Yang Zhao,[d] Lei Zhang,[*ab] Peihua Zhang,[a] Zefu Ye,[e] Zhujun Zhu,[e] Wangbao Yin*[ab] and Suotang Jia[ab]

Rapid and stable analysis of coal quality for fine management of coal is essential for the clean and efficient utilization of coal in thermal power plants. In this work, a software-controlled coal analyzer with laser-induced breakdown spectroscopy (LIBS) coupled with X-ray fluorescence spectroscopy (XRF) was developed, which includes an LIBS analysis module, XRF analysis module, sample feeding module, control module and operating software. The instrument not only plays to the strengths of LIBS in multi-element analysis, but also inherits the advantages of XRF in high stability analysis, so that it can be used in power plants for rapid and continuous quality analysis of coal tablets. Based on chemometric regression methods using principal component analysis (PCA) and partial least squares regression (PLS), as well as the spectra of hundreds of coal samples, quantitative prediction models were established, and the industrial test and performance evaluation of the instrument were completed in the Shanxi Yangguang Power Plant in China. The experimental results showed that the R^2 of the prediction models for calorific value, ash, volatiles and sulfur were 0.973, 0.986, 0.977 and 0.979, respectively, the RMSEs were 0.26 MJ kg^{-1}, 0.68%, 0.33% and 0.13%, respectively, the RMSEPs were 0.62 MJ kg^{-1}, 1.46%, 0.23% and 0.19%, respectively, and the average SDs were 0.11 MJ kg^{-1}, 0.49%, 0.15% and 0.09%, respectively. The models showed good accuracy and stability, and the repeatability of the measurements of coal quality all met the requirements of national standards, and thus, could meet the needs of power plants. This work provides a new idea for the increasingly mature application of LIBS in coal analysis in various industrial sites.

Received 11th January 2023
Accepted 9th May 2023

DOI: 10.1039/d3ja00015j

rsc.li/jaas

1 Introduction

Coal occupies a very important position in China's energy structure, which is determined by its resource endowment of "coal-rich, oil-poor and gas-poor". The data from China's National Bureau of Statistics[1] shows that the national raw coal production in 2021 is 4.13 billion tons, which was up 5.7% year-on-year. With a total energy consumption which was 5.2% higher than that of the previous year, of which, coal consumption was 2.934 billion tons of standard coal, coal consumption accounted for 56% of the total energy consumption. Meanwhile, China's power generation in 2021 was 8534.25 billion kW h, up 9.7% year-on-year. Thermal power generation was 580 580.87 billion kWh, up 8.9% year-on-year, with thermal power accounting for 68% of the total power generation. This shows that for some time in the future, and even longer term, coal will still play a fundamental role in ensuring China's energy security. However, with the implementation of China's energy conservation and emission reduction, low-carbon environmental protection, energy transformation policy, improving the clean and efficient use of coal has become a top priority. The clean and efficient utilization of coal mainly depends on the coal blending and combustion optimization of the thermal power plants. In China, due to the large number of coal types and variations in coal quality, it is easy to have a mismatch between the actual coal used in thermal power plants and the design coal used in its boilers, thus reducing the combustion efficiency of the boilers.

The key to achieving optimal control of coal blending and combustion in the thermal power plant is to realize the rapid analysis of coal quality, but at present, the power plants still generally use the traditional manual assay method.[2–4] Although these traditional chemical analysis methods are mature, accurate and stable, and the instruments and reagents have been widely used, their analytical processes are complicated and

[a]State Key Laboratory of Quantum Optics and Quantum Optics Devices, Institute of Laser Spectroscopy, Shanxi University, Taiyuan 030006, China. E-mail: k1226@sxu.edu.cn; ywb65@sxu.edu.cn

[b]Collaborative Innovation Center of Extreme Optics, Shanxi University, Taiyuan 030006, China

[c]Research Institute of Petroleum Processing, SINOPEC, Beijing 100089, China

[d]North University of China, Taiyuan 030051, China

[e]Shanxi Gemeng US-China Clean Energy R&D Center Co., Ltd, Taiyuan 030032, China

time-consuming. Therefore, it is not possible to analyze the quality of coal entering the plant per vehicle and analyze online the coal entering the furnace, as well as to improve the industrial production process. Although the newly developed robotic assay system has replaced manual labor with robots, the test method used has not changed, which is also time-consuming, bulky and expensive. The commercial neutron activation online analysis method has a problem of radioactive contamination. Therefore, the development of a low-cost rapid coal quality analyzer is a major demand from the thermal power plants.

Laser-induced breakdown spectroscopy (LIBS) is one of the most promising techniques for coal analysis due to its advantages of real-time, online, rapid, safe and simultaneous detection of multiple elements.[5] The composition of the sample is determined by analyzing the radiation spectrum of the plasma generated by the high-energy pulse laser. In recent years, there are many reports on coal quality analysis by LIBS. Yao *et al.*[6] combined cluster analysis, artificial neural networks (ANNs), and genetic algorithms (GA) to analyze the LIBS spectra of pulverized coal, and the mean standard deviation (SD) of the calorific value was 0.86 MJ kg^{-1}. Lu *et al.*[7] also used the spectral analysis method of ANNs combined with GA to conduct LIBS analysis on the calorific value of coal, with an SD of 0.38 MJ kg^{-1}. Li *et al.*[8] further reduced the SD of the coal calorific value to 0.22 MJ kg^{-1} by selecting variables through partial least squares (PLS) regression. The LIBS developed by Body and Chadwick[9] can simultaneously determine the elemental contents of Al, C, Ca, Fe, H, K, Mg, Na, and Si, in coal with a measurement repeatability of ±10%. Wang *et al.*[10] analyzed the deviation of the spectra using the mutual interference between the elements, and the mechanism of matrix effect, and the relative standard deviations (RSDs) of calibration and prediction were 5.79% and 8.10%, respectively. Li *et al.*[11] optimized the experimental parameters, and the minimum RSDs of Al, C, Ca, Fe, H, K, Mg, Na, and Si, in coal reached 4.66%, 4.10%, 3.14%, 3.73%, 4.45%, 4.21%, 4.91%, 2.34%, and 4.35%, respectively. Feng *et al.*[12] proposed a PLS model with multivariate dominant factors to analyze the amount of C in coal, and the root mean square error (RMSE) of the prediction was 2.92%. We have designed a fully software-controlled LIBS system,[13] and the RSD for measuring C in coal was 1.49%. Hou *et al.*[14] measured the caking index (G) and the maximum thickness of the plastic layer (Y) of coal using LIBS based on the PLS model of multi-variant dominant factors, where the RMSEs of the prediction of the G and Y values were relatively improved by 17.9% and 34.7%, respectively. Nevertheless, is still difficult to meet the requirements of national standards for the measurement repeatability of LIBS for the coal calorific value, ash content and other indicators.[15–17] This is due to the Rayleigh–Taylor instability of LIBS, the inherent energy fluctuation of the pulsed laser, the poor representativeness caused by the small focus point, and the instability of plasma due to external disturbances, which limit the measurement repeatability of LIBS.[18–20] How to break through the bottleneck of the measurement repeatability of the coal quality, becomes the key to determining whether LIBS can be successfully applied to the coal industry.

The X-ray fluorescence spectrometry (XRF) has shown good repeatability in coal quality analysis. The SD of ash in coal is only 1.7–2.5%,[21,22] and the measurement repeatability of the ash forming elements such as Al, Ca, Fe, K, Mg, Na, Si and Ti is far superior to that required by the national standards.[23] The principle of XRF is that when a single atom of an element is excited by external energy, it will emit a secondary X-ray fluorescence with characteristic energy (energy-dispersive XRF, ED-XRF) or wavelength (wavelength-dispersive XRF, WD-XRF), and the element can be quantitative analyzed according to the fluorescence intensity.[24] The XRF has a low fluorescence yield, and a sensitivity for elements with low atomic numbers,[25] and the corresponding detection limit is generally 50 μg g^{-1}, but it is 5 μg g^{-1} for elements with high atomic numbers. In this way, ED-XRF is only suitable for determining inorganic ash forming elements with atomic numbers larger than 11, but it cannot determine organic elements such as C and H in coal, so it cannot determine the calorific value and volatile matter of coal.

In summary, LIBS has low measurement repeatability but can analyze all the key elements in coal, whereas XRF can only analyze the ash forming elements but has excellent stability. The combination of the two methods can not only measure organic elements in coal, but also measure the inorganic elements with high stability, thus forming a new coal quality analysis method with high measurement repeatability. We have previously used a chemometric regression algorithm combining principal component analysis (PCA) and PLS in experiments to verify the feasibility of this method,[26–28] and the measurement repeatability of the coal calorific value has met the requirements of national standard. It is worth mentioning that PCA is an unsupervised learning method that can not only adjust the combination of multivariate data information to extract fewer integrated variable features to explain most of the information obtained from the original data, but can also reduce the dimensionality of the high-dimensional data space by using the principle of minimal loss of data information. However, the dependent variable is not involved in guiding the construction of the principal components in the process of dimensionality reduction by PCA, therefore, PCA cannot guarantee that the directions of the predictor variables can be well explained, whereas the dependent variable can be predicted satisfactorily.[29–31] The PLS is a supervised approach that incorporates the ideas of PCA, typical correlation analysis, and multiple linear regression. It not only enables the feature variables obtained after extraction to satisfactorily summarize the information of the original variables, but it also has a strong explanatory capability for the dependent variable. The PLS method obtains the mutually orthogonal eigenvectors of the independent and dependent variables by projecting the high dimensional data space of the independent and dependent variables into the corresponding low-dimensional space, and then establishes a univariate linear regression relationship between the eigenvectors of the independent and dependent variables. Not only can it overcome the covariance problem, it emphasizes the explanatory and predictive effects of the

independent variables on the dependent variable when selecting the eigenvectors, removes the influence of unhelpful noise on the regression, and ensures that the model contains the minimum number of variables.[32–34]

In this research discussed herein, we further developed an LIBS-XRF analyzer that combines PCA and PLS regression methods for coal quality measurement, and carried out industrial testing in a power plant to verify its performance.

2 Experimental

2.1 Experimental setup

Fig. 1 shows the image, 3D mechanical model, and schematic diagram of the LIBS-XRF analyzer, which is composed of an LIBS module, an XRF module, a sample delivery module, a control module and the operating software. The LIBS and XRF modules are encapsulated in an aluminum shell, which is mounted inside the box, with rubber pads between the aluminum shell and the inner wall of the box to give anti-vibration protection. All the modules are described in detail in the next sections.

(1) The LIBS module. The 3D model and schematic diagram of the module are shown in Fig. 2, which mainly includes a laser (M-NANO), beam expander (BE), half-wave plate ($\lambda/2$), polarization beam splitter (PBS), energy meter (EM), focusing lens (FL), concave mirror (CO), coupling lens (L), optical fiber, spectrometer (AvaSpec-ULS4096CL-EVO, Avantes, The Netherlands) and dust removal fan. The emitted laser beam with

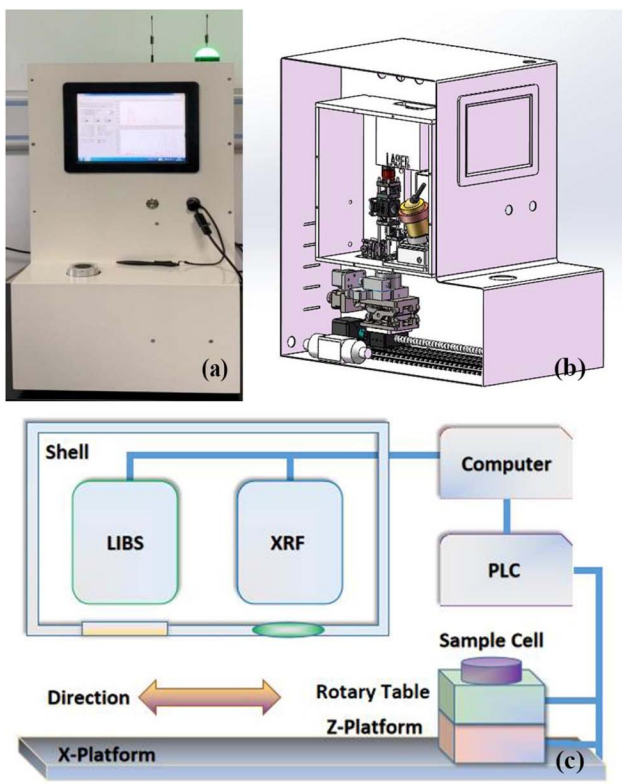

Fig. 1 (a) Image, (b) 3D mechanical model and (c) schematic diagram of the LIBS-XRF analyzer for coal quality measurement.

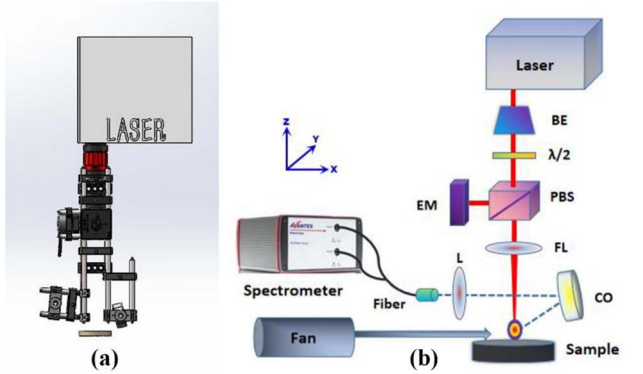

Fig. 2 (a) 3D mechanical model and (b) schematic diagram of the LIBS module.

a wavelength of 1064 nm, energy of 60 mJ, pulse width of 8 ns, and repetition frequency of 6 Hz was divided into two beams after passing through the 2× BE, half-wave plate, and PBS. The reflected laser beam was received by the EM, and the transmitted laser beam was focused on the surface of the coal sample by the FL, with a focal length 100 mm, to form a plasma. The radiated fluorescence was collected by a UV-enhanced concave mirror with a focal length of 50 mm, coupled to the optical fiber by a quartz plano-convex lens with a focal length of 30 mm, and then introduced into the spectrometer. Here, the beam expander not only prevented the high-power laser from damaging the optical components, but also reduced the divergence angle and diffraction effect of the laser to ensure good alignment. The $\lambda/2$ plate and PBS were used to adjust the energy ratio of the transmitted and reflected laser beams. The wavelength ranges of the dual-channel spectrometer were 195–321 nm and 496–732 nm, and the corresponding spectrum resolution was 0.15 nm, and the minimum integration time was 1.05 ms. The dust removal fan was used to suck away the pulverized coal generated during the measurement.

(2) The XRF module. The structure of the ED-XRF module is shown in Fig. 3, and is composed of an X-ray tube (VF-50J, Varex Imaging, USA), silicon drift detector (SDD, DV H20, Ketek, Germany), vacuum chamber, beryllium window (BW), collimator (CM), high-voltage power supply (MNX 50W), digital pulse processor (DPP), vacuum pump (VP, SVF-E1, Scroll Labs, USA) and vacuum gauge (VG, APG-500). The X-ray tube and SDD were placed on both sides of the chamber at an angle of 45°. The X-ray tube was connected to the high-voltage power supply, and the SDD was connected to the DPP, and the sample was located 2 mm below the BW. During the measurement, the primary X-ray emitted irradiated the sample surface after passing through the CM and BW, and the X-ray fluorescence generated was detected by the SDD and transmitted to the computer after being processed by the DPP. In order to prevent the detection window from being polluted by dust, the module uses a top illuminated structure. The tube voltage and current of the high-voltage power supply were 10 kV and 0.25 mA, respectively, and the peak time of the SDD was 4.8 μs. The vacuum of the chamber was maintained at 100 Pa, and its bottom plate was

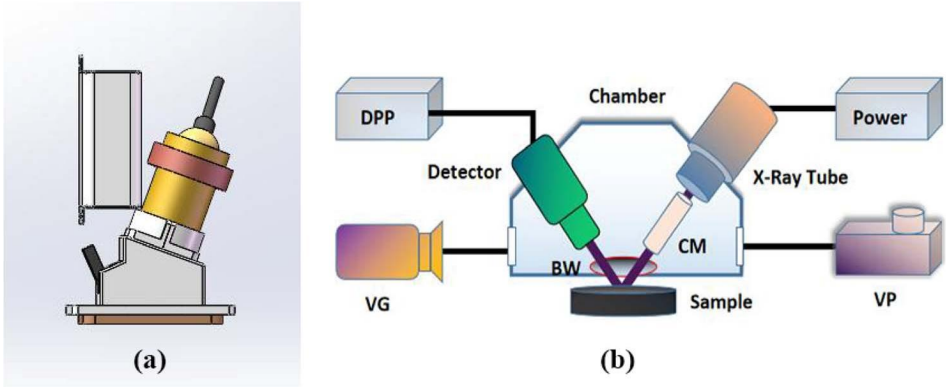

Fig. 3 (a) 3D mechanical model, and (b) schematic diagram of the XRF module. DPP: digital pulse processor, BW: beryllium window, CM: collimator, VG: vacuum gauge, VP: vacuum pump.

made of brass to avoid interference with the coal quality measurement.

(3) Sample delivery module. This module was located below the LIBS and XRF modules, and its 3D mechanical model is shown in Fig. 4. From bottom to top are the *X*-axis translation table, *Z*-axis translation table, rotation table and sample cell. The *X*-axis translation table is a double-track sliding table with a length of 400 mm, which was used to control the horizontal movement of the sample. The *Z*-axis translation table is a shear type lifting structure to precisely control the distance between the sample surface and the BW. The rotary table is driven by a worm gear and was used to control the rotation of the sample. The 3D mechanical model of the sample cell is shown in Fig. 5, which is used to hold the coal tablet. The slots on both sides of the cell are convenient for taking samples.

(4) Control module. The module is used to control the timing of the whole instrument and spectral analysis, including the computer, programmable logic controller (PLC, 224XP), relays, drivers, photoelectric switches, and so on. Here, the PLC is used for timing control, and the relays are used to control the switching on and off of each component, the drivers are used to drive the tables, and the photoelectric switches are used for positioning.

(5) Operating software. The software used was LabVIEW (National Instruments, USA), and the user interface is shown in Fig. 7. The left side is used to set the control parameters, and the right side displays the spectra and analysis results.

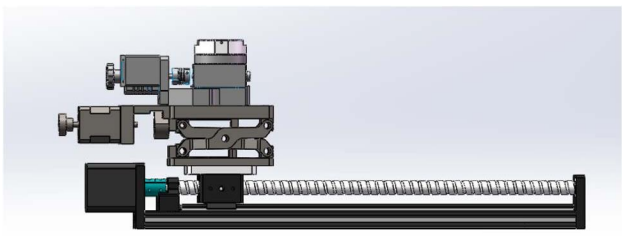

Fig. 4 The 3D mechanical model of the sample delivery module.

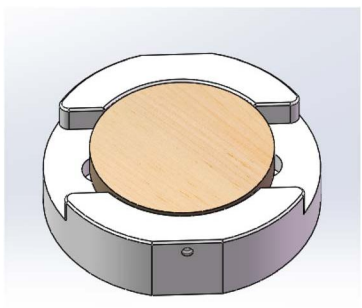

Fig. 5 The 3D mechanical model of the sample cell.

2.2 Workflow

The operating process of the developed analyzer is as follows. First, the start measurement button was clicked, and the

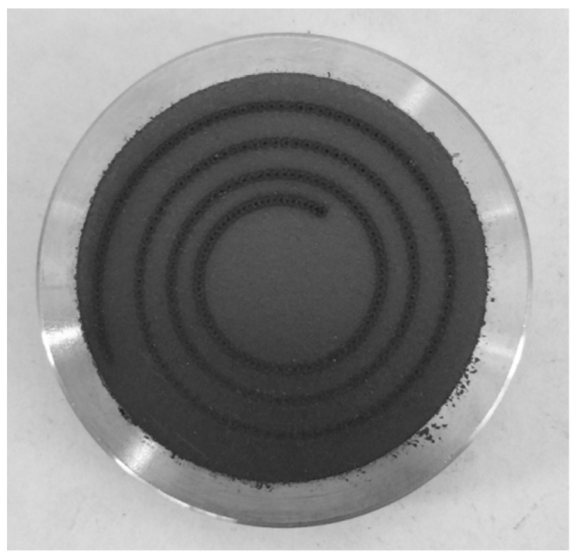

Fig. 6 The spiral path of laser ablation on the surface of the coal tablet.

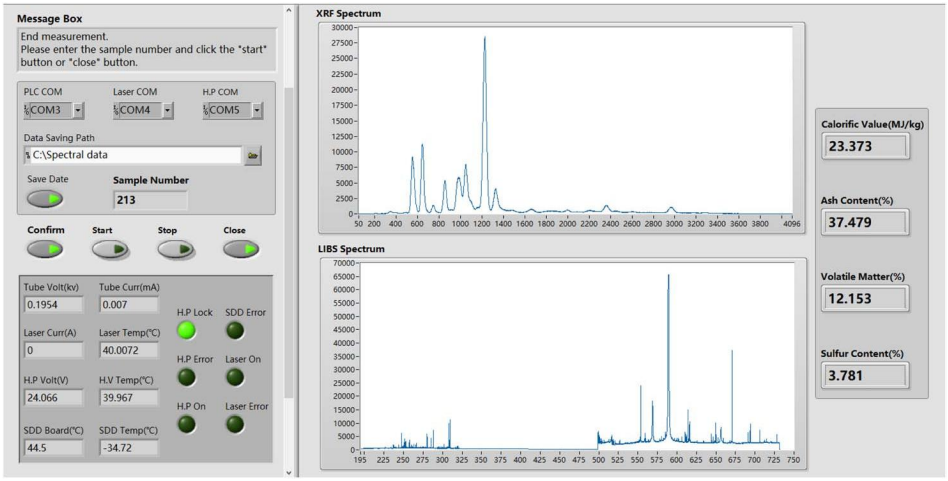

Fig. 7 The user interface of the LabVIEW operating software.

sample cell first descends to the specified height, then moves to the bottom of the XRF module and rotates at 1 r/min. The amount of vacuum of the chamber is maintained after it is reduced to 100 Pa. At this time, the X-ray tube and the SDD start working, and the XRF measurement is completed 1 min later. After that, the sample cell continues to move to the bottom of the LIBS analysis module, then the dust fan starts, and the LIBS measurement starts and then ends 1 min later. Finally, the sample pool quickly returned to the initial position, and the software interface displayed the quantitative results. In the LIBS measurement, by setting a reasonable speed for the rotary table and the *X*-axis translation table, the laser ablation points on the sample surface show a spiral path (Fig. 6), and this increases the distance between the points, ensuring that the laser ablation point is new at the time of measurement.

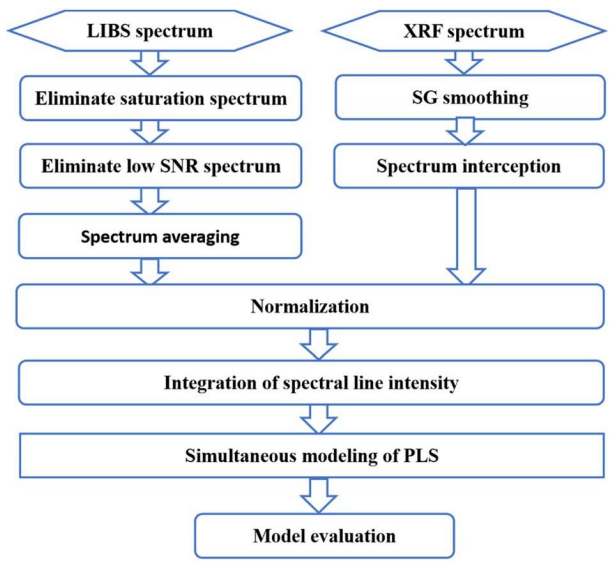

Fig. 8 The analysis process for the spectral data.

2.3 Samples

In this experiment, 334 air dried coal samples with an average particle size of 200 μm, and the corresponding standard data were provided by the Shanxi Yangguang power plant. These pulverized coal samples were all pressed into tablets with a diameter of 40 mm and a thickness of 6 mm under a pressure of 30 MPa (Fig. 6). A total of 318 samples were used as a training set for modeling, and the remaining 16 samples were used as a validation set. Each sample in the validation set was tested five times to evaluate the measurement repeatability.

2.4 Spectral analysis

The whole analysis process of spectral data is shown in Fig. 8, and mainly includes spectral pretreatment, modeling and model evaluation. The details are as follows:

(1) Spectral pretreatment. For the LIBS spectra, the pretreatment methods (Fig. 9) include removing saturated spectra, removing low signal-to-noise ratio (SNR) spectra, averaging and normalization. Here, saturated spectrum refers to a spectrum whose spectral line intensity exceeds the range of the spectrometer. The removal of low signal-to-noise ratio (SNR)

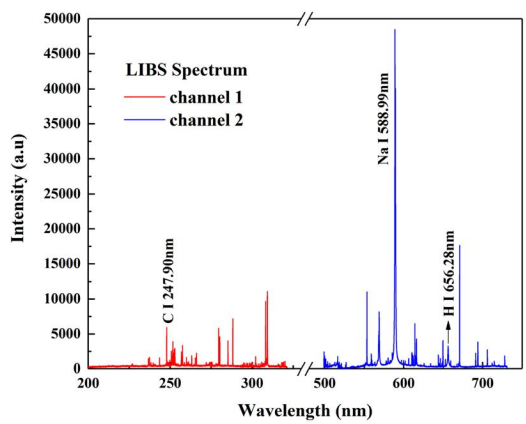

Fig. 9 Typical LIBS spectrum of coal.

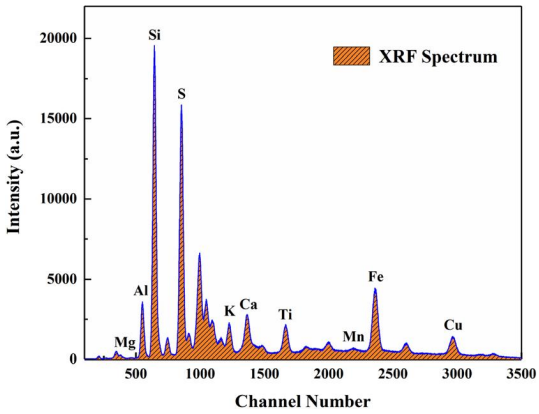

Fig. 10 Typical XRF spectrum of coal.

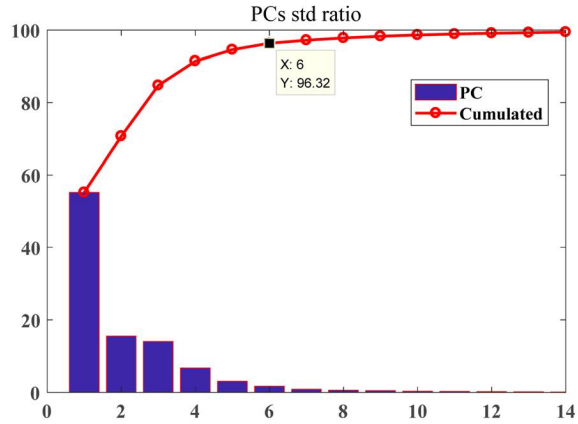

Fig. 12 The PCA of the LIBS spectrum.

spectra is done by first calculating the SNR of the element-specific spectral lines in each remaining spectrum, then sorting the spectra by SNR size, and finally rejecting 10% of the low SNR spectra. Normalization is done by subtracting the minimum value in the average spectrum and then dividing it by the maximum value in the processed spectrum.

For the XRF spectra (Fig. 10), the pretreatment methods include Savitzky–Golay (SG) smoothing, interception and normalization. Here, the SG smoothing uses five-point, third-order smoothing. Interception is used to remove the invalid spectral segments and to leave the effective spectra. The normalization method is consistent with LIBS for the elimination of the magnitude difference between the LIBS and XRF data. Based on the results of previous spectral line selection,[26] the C, H, Na lines in the LIBS spectrum and the Al, Ca, Fe, K, Mg, Mn, S, Si, Ti, lines in the XRF spectrum were directly selected for the following modeling.

(2) Modeling. Combining the spectra after pretreatment and the standard data of the coal samples, the principal components were selected by PCA, and then the prediction model of coal quality was established using PLS. Considering that the coal quality is closely related to the content of each element in the coal, and that the LIBS spectrum had interference from the "matrix effect" and the "self-absorption effect",[35] multiple spectral lines were selected as the initial input variables for the modeling. Firstly, the principal components of the input

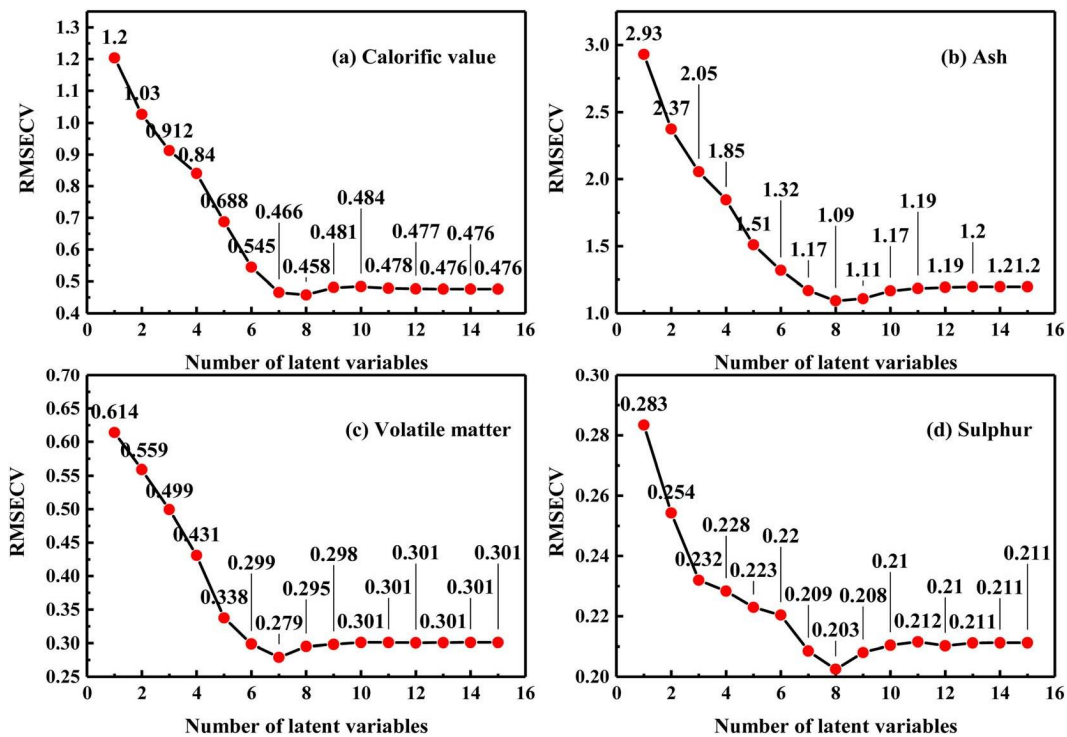

Fig. 11 The RMSECV *vs.* latent variables plot for each PLS model.

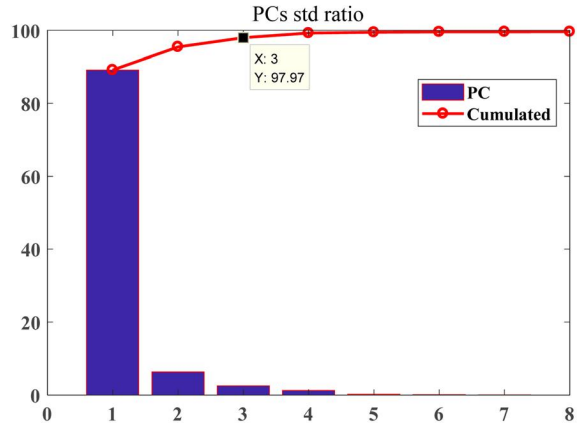

Fig. 13 The PCA of the XRF spectrum.

variables were extracted to eliminate redundant variables and reduce the array dimension, and then the regression model was established using the standard data of the coal samples and the extracted principal components. For the calorific value, it was not only positively correlated with C, H and S, but also negatively correlated with ash content, so the Al, C, Ca, Fe, H, K, Mg, Mn, Na, S, Si, and Ti, lines were selected as the initial input variables of the prediction model of calorific value. The ash content was mainly related to the inorganic elements in coal, so the Al, Ca, Fe, K, Mg, Mn, Na, Si, and Ti, lines were selected as the initial input variables. For volatile matter, in addition to organic elements, the C, H and S lines, the spectral lines of some other elements with a high correlation were selected as input vectors. For the sulfur content, the spectral lines of S and other interfering elements were taken as the initial input variables. Due to the different elemental spectra selected for the four coal quality indicators, the numbers of principal components were also different. To reduce the influence of the secondary components, the final numbers of principal components selected at a 95% confidence interval by PCA were 12, 11, 9 and 9. The 10-fold cross-validation and 15-fold Monte Carlo cross-validation were used to obtain the optimal parameters when building the PLS model, to avoid overfitting as much as possible, and to test the performance of the model on unfamiliar data sets. After recalculation and further optimization, the number of latent variables selected for each PLS model was finally determined to be 8, 8, 7, and 8, which were chosen by the root mean square error of cross-validation (RMSECV) parameters and the latent variable relationship diagram (Fig. 11) of each PLS model.

Table 1 Performance evaluation of the coal quality prediction model using data obtained from the PLS

Coal quality	R^2	RMSE	RMSEP	SD	GB[a]
Calorific value (MJ kg^{-1})	0.973	0.26	0.62	0.11	0.12
Ash content (%)	0.986	0.68	1.46	0.49	0.50
Volatile matter (%)	0.977	0.33	0.23	0.15	0.30
Sulfur content (%)	0.979	0.13	0.19	0.09	0.10

[a] GB: National Standard of the People's Republic of China.

It should be noted that due to the large number of collected samples and the combination of LIBS spectra and XRF spectra,

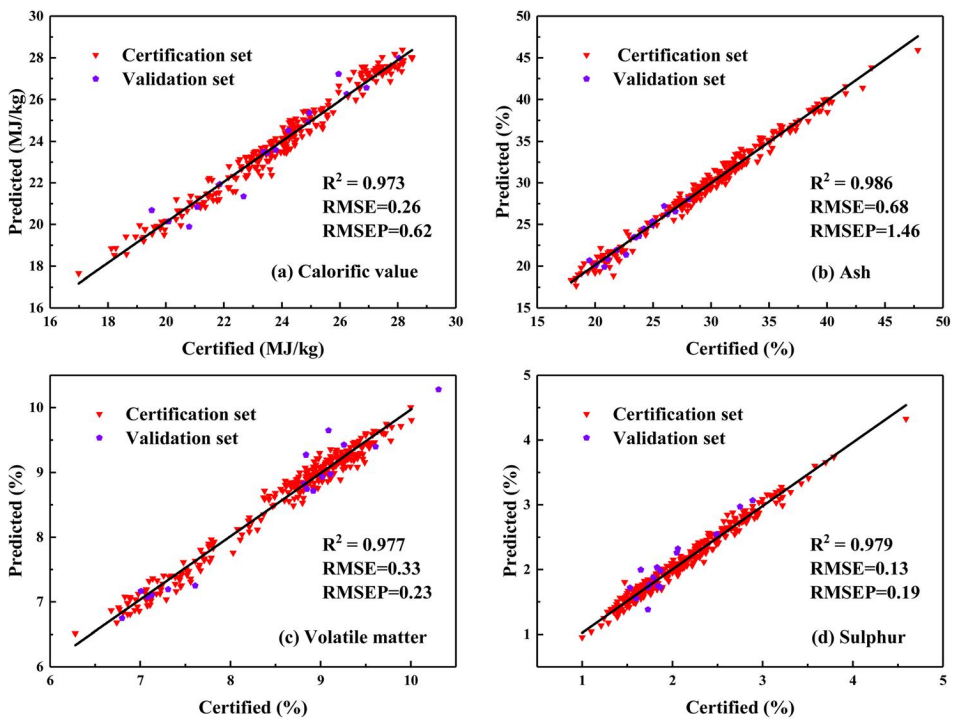

Fig. 14 Calibration results of the coal quality of samples in the training set obtained using the LIBS-XRF analyzer.

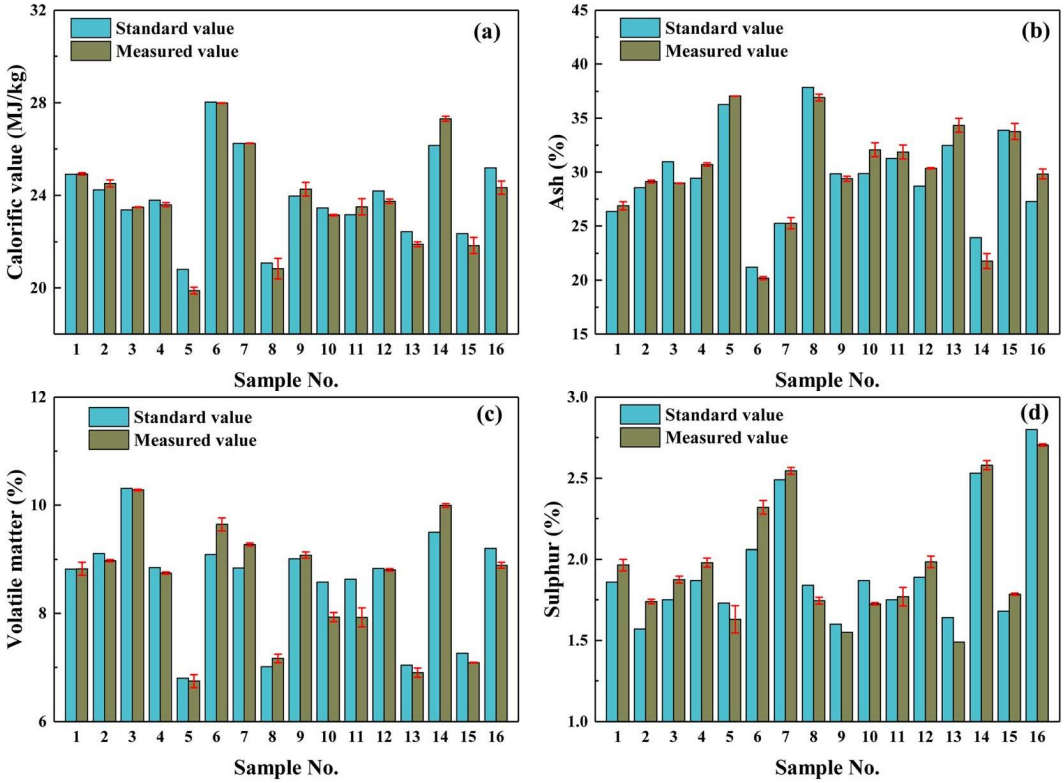

Fig. 15 Comparison between the predicted results of (a) calorific value, (b) ash content, (c) volatile matter and (d) sulfur content of 16 new coal samples and the standard data.

the amount of data used for mathematical modeling became very large. If the PLS method was used directly for modeling, the calculation process would be time-consuming and require a high computer performance. Moreover, the processing of data from the combined spectra itself was tedious. In this study, the modeling was based on PCA using the PLS method. There were two main purposes of using PCA, one was to eliminate the redundant variables in the original spectra and perform data dimensionality reduction, and the other was to select the variables that contributed more to each component by their loadings. After screening the spectra based on the PCA loadings, the PLS was used for mathematical modeling, which did not directly use the principal components of the PCA as input variables for PLS. Fig. 12 and 13 show the number of each principal component and their cumulative contribution to the respective spectra after PCA analysis of LIBS and XRF spectra, respectively.

(3) Model evaluation. The regression model was used to predict the calorific value, ash content, volatile matter and sulfur content of coal. Its accuracy was evaluated by the linear correlation coefficients (R^2) and RMSE, whereas its repeatability was evaluated by SD.

3 Results and discussion

The calibration results of the analysis of the coal quality of the coal samples in the training set are shown in Fig. 14. It can be seen that the model shows good correlation between the predicted values and the standard data, and all the values of R^2 were greater than 0.97. Table 1 lists the R^2 and RMSE values of the model for samples in the training set, the Root Mean Square Error of Prediction (RMSEP) and SD of the prediction in the validation set, and the SD specified in the national standards. It was seen that the LIBS-XRF analyzer had a good measurement accuracy and stability for coal quality, and the repeatability meets the national standard requirements.

To verify the actual performance of the analyzer, this instrument was field tested in the laboratory of the Shanxi Yangguang Power Plant for three months. A comparison between the prediction results of the coal quality of 16 new coal samples and the standard data is shown in Fig. 15. It can be seen that the average SDs of calorific value, ash content, volatile matter and sulfur content of this instrument were 0.11 MJ kg^{-1}, 0.49%, 0.15% and 0.09%, respectively, which meet the actual requirements of power plants.

4 Conclusions

In this work, we developed an LIBS-XRF coal quality analyzer based on the highly stable XRF assisted LIBS analysis method, which consists of an LIBS module, an XRF module, a sample delivery module, a control module and operating software. The analysis algorithm includes spectral pretreatment, PCA and PLS modeling. The instrument was applied in the Shanxi

Yangguang Power Plant for industrial testing and performance evaluation, and the prediction models used for coal quality analysis were established by using the spectra of hundreds of coal samples. The test results showed that the RMSEPs of the calorific value, ash content, volatile matter and sulfur content of coal were 0.62 MJ kg^{-1}, 1.46%, 0.23% and 0.19%, respectively, and the average SDs were 0.11 MJ kg^{-1}, 0.49%, 0.15% and 0.09%, respectively. The measurement repeatability meets the requirements of national standards. Next, the online analysis system will be further developed in combination with the sampler, crusher, grinder, and so on, to monitor the coal quality on the conveyor belt in real time.

Author contributions

Zhihui Tian was the main author, responsible for the instrument design, construction and software visualization programming, and wrote the first draft of the manuscript. Jiaxuan Li was responsible for the commissioning of the apparatus and the testing of the experimental data. Shuqing Wang organized the database. Yu Bai was responsible for the automation programming and control of the instrument. Yang Zhao performed the statistical analysis of the data. Lei Zhang and Wangbao Yin contributed to the conception and design of the study, and reviewed and revised the manuscript. Peihua Zhang, Zefu Ye, Zhujun Zhu, and Suotang Jia provided suggestions to improve the manuscript and supported the testing of the instrumentation. All the authors reviewed and commented on the subsequent versions of the manuscript, and read and approved the final manuscript.

Conflicts of interest

There are no conflicts of interest to declare.

Acknowledgements

This work is supported by the National Energy R&D Center of Petroleum Refining Technology of China (RIPP, SINOPEC), the National Key Research and Development Program of China (Grant No. 2017YFA0304203), the Changjiang Scholars and Innovative Research Team in the University of Ministry of Education of China (Grant No. IRT_17R70), the National Natural Science Foundation of China (NSFC) (Grant Nos. 61975103 and 61875108), the Industrial Application Innovation Project (Grant No. 627010407), the Scientific and Technological Innovation Project of Shanxi Gemeng US-China Clean Energy R&D Center Co., Ltd, the 111 Project (D18001), and the Fund for Shanxi "1331KSC".

References

1 K. Liu, C. He, C. Zhu, J. Chen, K. Zhan and X. Li, *TrAC, Trends Anal. Chem.*, 2021, **143**, 116357.
2 D. M. Mason and K. N. Gandhi, *Fuel Process. Technol.*, 1983, **7**, 11–22.
3 A. White and J. Whittingham, *Fuel*, 1983, **62**, 1058–1061.
4 C. J. Donahue and E. A. Rais, *J. Chem. Educ.*, 2009, **86**, 222.
5 S. Sheta, M. S. Afgan, Z. Hou, S.-C. Yao, L. Zhang, Z. Li and Z. Wang, *J. Anal. At. Spectrom.*, 2019, **34**, 1047–1082.
6 S. Yao, J. Mo, J. Zhao, Y. Li, X. Zhang, W. Lu and Z. Lu, *Appl. Spectrosc.*, 2018, **72**, 1225–1233.
7 Z. Lu, J. Mo, S. Yao, J. Zhao and J. Lu, *Energy Fuels*, 2017, **31**, 3849–3855.
8 W. Li, M. Dong, S. Lu, S. Li, L. Wei, J. Huang and J. Lu, *Anal. Methods*, 2019, **11**, 4471–4480.
9 D. Body and B. L. Chadwick, *Rev. Sci. Instrum.*, 2001, **72**, 1625–1629.
10 D. Wang, J. Liu, M. Dong, S. Yao, J. Fan, Z. Tian, L. Wang and S. Li, *Spectrosc. Spectral Anal.*, 2016, **36**, 2607–2612.
11 J. Li, J. Lu, Z. Lin, S. Gong, C. Xie, L. Chang, L. Yang and P. Li, *Opt. Laser Technol.*, 2009, **41**, 907–913.
12 J. Feng, Z. Wang, L. West, Z. Li and W. Ni, *Anal. Bioanal. Chem.*, 2011, **400**, 3261–3271.
13 W. Yin, L. Zhang, L. Dong, M. Weiguang and S. Jia, *Appl. Spectrosc.*, 2009, **63**, 865–872.
14 Z. Hou, Z. Wang, L. Li, X. Yu, T. Li, H. Yao, G. Yan, Q. Ye, Z. Liu and H. Zheng, *Spectrochim. Acta, Part B*, 2022, **191**, 106406.
15 National Standard of the People's Republic of China, *Standards Determination of calorific value of coal*, **https://www.doc88.com/p-2085950523399.html**, accessed December 2022.
16 National Standard of the People's Republic of China, *Standards Proximate analysis of coal*, **https://www.doc88.com/p-9426174796634.html?r=1**, accessed December 2022.
17 National Standard of the People's Republic of China, *Standards Determination of total sulfur in coal*, **https://www.doc88.com/p-7894829171176.html**, accessed December 2022.
18 T. Labutin, A. Popov, S. Raikov, S. Zaytsev, N. Labutina and N. Zorov, *J. Appl. Spectrosc.*, 2013, **80**, 315–318.
19 Y.-T. Fu, W.-L. Gu, Z.-Y. Hou, S. A. Muhammed, T.-Q. Li, Y. Wang and Z. Wang, *Front. Phys.*, 2021, **16**, 1–10.
20 Y. Fu, Z. Hou, T. Li, Z. Li and Z. Wang, *Spectrochim. Acta, Part B*, 2019, **155**, 67–78.
21 S. Uffelmann, *Nucl. Instrum. Methods Phys. Res., Sect. A*, 1986, **242**, 550–557.
22 M. Mujuru, R. McCrindle, B. Botha and P. P. Ndibewu, *Fuel*, 2009, **88**, 719–724.
23 D. Hicks, J. O'Reilly and D. Kopenaal, *AIP Conf. Proc.*, 1981, **70**, 454–455.
24 K. Ma, *Coal Quality Technology*, 2019, **2**, 32–35.
25 F. Li, L. Meng, W. Ding, J. Wang and L. Ge, *X-Ray Spectrom.*, 2022, **51**, 346–364.
26 X. Li, L. Zhang, Z. Tian, Y. Bai, S. Wang, J. Han, G. Xia, W. Ma, L. Dong and W. Yin, *J. Anal. At. Spectrom.*, 2020, **35**, 2928–2934.

27 Y. Bai, J. Li, W. Zhang, L. Zhang, J. Hou, Y. Zhao, F. Chen, S. Wang, G. Wang and X. Ma, *Front. Phys.*, 2022, **9**, 820.
28 T. Zhihui, L. Xiaolin, W. Gang, L. Zhang, L. Jiaxuan, W. Shuqing, B. Yu, W. Zhang, Y. Han and M. Xiaofei, *Plasma Sci. Technol.*, 2022, **24**, 084007.
29 A. Daffertshofer, C. J. Lamoth, O. G. Meijer and P. J. Beek, *Clin. Biomech.*, 2004, **19**, 415–428.
30 H. Abdi and L. J. Williams, *Wiley Interdiscip. Rev. Comput. Stat.*, 2010, **2**, 433–459.
31 S. Karamizadeh, S. M. Abdullah, A. A. Manaf, M. Zamani and A. Hooman, *J. Signal Process. Syst.*, 2013, **4**, 173.
32 J. F. Hair, J. J. Risher, M. Sarstedt and C. M. Ringle, *Eur. Bus. Rev.*, 2019, **31**, 2–24.
33 J. Hulland, *Strateg. Manag. J.*, 1999, **20**, 195–204.
34 S. Wold, M. Sjöström and L. Eriksson, *Chemom. Intell. Lab. Syst.*, 2001, **58**, 109–130.
35 J. Hou, L. Zhang, Y. Zhao, W. Ma, L. Dong, W. Yin, L. Xiao and S. Jia, *Opt. Express*, 2019, **27**, 3409–3421.